Nat Med. Author manuscript; available in PMC 2013 October 01.

Published in final edited form as:
Nat Med. 2012 October ; 18(10): 1575–1579. doi:10.1038/nm.2897.

Sarcolipin is a newly identified regulator of muscle-based thermogenesis in mammals

Naresh C Bal[1], **Santosh K Maurya**[1,5], **Danesh H Sopariwala**[1,5], **Sanjaya K Sahoo**[1], **Subash C Gupta**[1], **Sana A Shaikh**[1], **Meghna Pant**[1], **Leslie A Rowland**[1], **Eric Bombardier**[2], **Sanjeewa A Goonasekera**[3], **A Russell Tupling**[2], **Jeffery D Molkentin**[3], and **Muthu Periasamy**[1,4]

[1]Department of Physiology and Cell Biology, Ohio State University, College of Medicine, Columbus, Ohio, USA

[2]Department of Kinesiology, Faculty of Applied Health Sciences, University of Waterloo, West Waterloo, Ontario, Canada

[3]Howard Hughes Medical Institute, Molecular Cardiovascular Biology, Cincinnati Children's Hospital Medical Center, Cincinnati, Ohio, USA

[4]Davis Heart and Lung Research Institute, Ohio State University, Columbus, Ohio, USA

Abstract

The role of skeletal muscle in nonshivering thermogenesis (NST) is not well understood. Here we show that sarcolipin (Sln), a newly identified regulator of the sarco/endoplasmic reticulum Ca^{2+}-ATPase (Serca) pump[1–5], is necessary for muscle-based thermogenesis. When challenged to acute cold (4 °C), *Sln*$^{-/-}$ mice were not able to maintain their core body temperature (37 °C) and developed hypothermia. Surgical ablation of brown adipose tissue and functional knockdown of Ucp1 allowed us to highlight the role of muscle in NST. Overexpression of Sln in the Sln-null background fully restored muscle-based thermogenesis, suggesting that Sln is the basis for Serca-mediated heat production. We show that ryanodine receptor 1 (Ryr1)-mediated Ca^{2+} leak is an important mechanism for Serca-activated heat generation. Here we present data to suggest that Sln can continue to interact with Serca in the presence of Ca^{2+}, which can promote uncoupling of the Serca pump and cause futile cycling. We further show that loss of *Sln* predisposes mice to diet-induced obesity, which suggests that Sln-mediated NST is recruited during metabolic overload.

Correspondence should be addressed to M. Periasamy (periasamy.1@osu.edu).
[5]These authors contributed equally to this work.

Note: Supplementary information is available in the online version of the paper.

AUTHOR CONTRIBUTIONS

M. Periasamy and N.C.B. conceived of the study idea and designed the experiments. D.H.S., S.A.S., M. Pant and L.A.R. designed and conducted mouse breeding. S.K.M., N.C.B., D.H.S. and M. Pant performed the thermogenesis experiments. N.C.B., S.C.G. and S.K.M. conducted HFD feeding experiments. S.K.S. designed and conducted chemical crosslinking studies. E.B. designed and conducted HFD experiments on *Sln*$^{-/-}$ mice. A.R.T. conceived the idea of and designed the HFD studies. S.A.G. and J.D.M. generated and characterized the Sln overexpression mouse model. M. Periasamy, S.K.M., S.K.S., N.C.B. and D.H.S. analyzed the data and assembled the figures. M. Periasamy, N.C.B. and D.H.S. wrote the manuscript.

COMPETING FINANCIAL INTERESTS

The authors declare no competing financial interests.

These data collectively suggest that SLN is an important mediator of muscle thermogenesis and whole-body energy metabolism.

Endothermic animals require heat production from within to maintain their core temperature. Mammals, including humans, depend on both shivering and NST mechanisms for temperature homeostasis[6,7]. Although muscle shivering is an immediate response to cold stress, continuous muscle shivering leads to exhaustion and muscle damage; therefore, NST mechanisms are activated in these conditions. Brown adipose tissue (BAT) is an important site of NST in most mammals[8–10]. Several studies have suggested that in addition to BAT, skeletal muscle has a role in NST[7,11,12], but the molecular details of its involvement have not been completely explored. Studies conducted on heater organs (modified ocular muscle)[13–16] of fish have shown that continuous sarcoplasmic reticulum Ca^{2+} transport (caused by an inherently leaky ryanodine receptor) has evolved for heat production without muscle contraction. Similarly, in malignant hyperthermia, mutations in Ryr1 predispose to abnormal Ca^{2+} leak when exposed to anesthetic compounds. This condition elevates the amount of cytosolic Ca^{2+} and results in excessive activation of Serca-mediated Ca^{2+} transport and heat production[17]. However, it is not currently known to what extent the sarcoplasmic reticulum Ca^{2+} transport machinery is recruited in muscle-based NST in the absence of contraction. Recent *in vitro* studies have suggested that Sln can increase heat production by uncoupling Serca-mediated ATP hydrolysis from Ca^{2+} transport[18,19]. In this study, we sought to determine whether the Sln-Serca interaction is an important mechanism for muscle-based thermogenesis *in vivo*.

The generation of the $Sln^{-/-}$ mouse model has been previously described[4]. Loss of Sln in this model enhances Serca activity and improves muscle function in the muscle tissues where it is expressed[4,20]. When housed at 22 ± 1.5 °C (mean ± range), $Sln^{-/-}$ mice had an optimal average core temperature of 36.8 ± 0.3 °C (mean ± s.e.m.) (Supplementary Fig. 1a) and surface body heat (Fig. 1a). Because BAT is an important contributor to NST in rodents, loss of Sln could be compensated for by BAT. Therefore, we surgically ablated intrascapular BAT (iBAT), which constitutes ≥60% of the total BAT content, in a set of wild-type (WT) and $Sln^{-/-}$ mice to minimize its contribution. At 22 ± 1.5 °C, removal of iBAT in WT and $Sln^{-/-}$ mice did not have a major effect on the core temperature (Fig. 1a and Suplementary Fig. 1a), physical activity (Supplementary Fig. 1b), oxygen consumption (VO_2) or respiratory exchange ratio of the mice (Supplementary Fig. 1c,d). These data show that $Sln^{-/-}$ mice can maintain an optimal core temperature at 22 ± 1.5 °C, suggesting that Sln-dependent NST is not activated under these conditions.

To determine whether Sln is important for cold-induced thermogenesis, we exposed $Sln^{-/-}$ mice to acute cold (4 °C) in a temperature-controlled Comprehensive Lab Animal Monitoring System (CLAMS) module and monitored their core temperature using an infrared camera and implantable transponders. Infrared imaging of $Sln^{-/-}$ mice challenged to a temperature of 4 °C showed a substantial reduction in surface body heat, as determined by a switch in heat intensity from red to yellow (Fig. 1a). When exposed for a prolonged period (10 h) to 4 °C, the iBAT-ablated $Sln^{-/-}$ mice, despite their skeletal muscle shivering (Supplementary Fig. 2a and Supplementary Video 1), could not maintain optimal core

temperature, and their average body temperature dropped drastically from 37 °C to 32.2 ± 1.4 °C after 4 h and then dropped to 26.9 ± 1.9 °C after 6 h (Fig. 1b). The iBAT-ablated *Sln*$^{-/-}$ mice died of hypothermia during 10 h of cold exposure; therefore, we removed the iBAT-ablated *Sln*$^{-/-}$ mice from cold exposure when their core temperature reached 25 °C (early removal criteria, ERC). More than 85% of the iBAT-ablated *Sln*$^{-/-}$ mice reached ERC (Fig. 1c). However, *Sln*$^{-/-}$ mice with intact iBAT maintained a lowered average core temperature of 33.8 ± 0.6 °C and survived cold challenge, suggesting that BAT can compensate for the loss of Sln. WT mice with intact iBAT were able to maintain an average core temperature of 36.3 ± 0.2 °C during cold challenge (close to the optimal core temperature of 37 °C), which is in agreement with published results[21]. Notably, iBAT-ablated WT mice were able to maintain their core temperature (35.8 ± 0.4 °C) and survive the cold challenge (Fig. 1b,c), suggesting that Sln-mediated NST can compensate for loss of iBAT.

We further evaluated the cold sensitivity (on challenge to 4 °C) of the *Sln*$^{-/-}$ mice in a group that we acclimatized for 3 weeks at 30 °C (thermoneutrality for mice) to functionally downregulate the activity of BAT[22,23]. We used this method instead of a double knockout for *Sln* and *Ucp1* because very few double knockout mice are born (below the Mendelian ratio), and those that survive to adulthood may develop additional compensatory mechanisms, complicating interpretations of the results (L.A.R. and M.P., unpublished data). The *Sln*$^{-/-}$ mice acclimatized to 30 °C showed a drastic drop in their average core temperature from 37 °C to 32.5 ± 0.6 °C, whereas *Sln*$^{-/-}$ mice maintained at 22 °C had average core temperatures that decreased from 37 °C to 35.0 ± 0.6 °C during the first hour of cold exposure (Fig. 1d,e). The average core temperature of WT littermates acclimatized at 30 °C decreased from 37 °C to 35.2 ± 0.4 °C in first hour of cold challenge (Fig. 1e), which suggests that Sln can compensate for reduced BAT function. These results, together with those from the iBAT ablation (Fig. 1b,c) studies, suggest that Sln-mediated muscle thermogenesis has a crucial role in the maintenance of core body temperature that is independent of BAT activity.

We further evaluated how the loss of Sln affected metabolic rates by measuring the VO_2 in WT and *Sln*$^{-/-}$ mice at 22, 30 and 4 °C. The WT and *Sln*$^{-/-}$ mice housed at 22 °C showed higher basal VO_2 (Fig. 1f,g) compared to the groups of mice maintained at 30 °C. When challenged to 4 °C, both WT and *Sln*$^{-/-}$ (both reared at 22 °C) showed comparable increases in VO_2; however, the *Sln*$^{-/-}$ mice acclimatized to 30 °C showed a blunted increase in VO_2 (with 17.2% lower final VO_2) compared to WT littermates (Fig. 1g). These data suggest that acclimatization at 30 °C reduces the contribution of BAT to metabolic rate, and mice lacking Sln that are acclimatized at 30 °C are unable to increase their metabolic rate when challenged to 4 °C as compared to WT mice.

To ascertain that the inability to maintain core temperature by *Sln*$^{-/-}$ mice during acute cold exposure is primarily caused by loss of Sln expression, we re-expressed Sln in the knockout mice. We achieved this rescue by mating a mouse model overexpressing Sln under the control of the skeletal α-actin promoter with the *Sln*$^{-/-}$ mice. This new mouse model (*Sln*$^{-/-/OE}$) had high expression of Sln in the skeletal muscles (Fig. 2a). Importantly, overexpression of Sln in the null background fully restored thermogenesis; the iBAT-ablated

Sln$^{-/-/OE}$ mice did not develop hypothermia during challenge to 4 °C (Fig. 2b). These data collectively suggest that Sln is essential for skeletal-muscle–based facultative thermogenesis.

In addition to shivering, skeletal-muscle–based NST has been suggested to have a crucial role in thermogenesis[6], but direct experimental evidence supporting this is lacking. To show that skeletal muscle is an important site of NST, we inhibited shivering in WT mice (C57BL/6J) by administering a low dose of curare (0.4 mg per kg body weight intraperitoneally[24]), which is known to competitively block the binding of the neurotransmitter acetylcholine to its receptors[25]. When exposed to cold, untreated WT mice with intact iBAT showed normal shivering and maintained an average core temperature of 36.3 ± 0.2 °C (Fig. 2c). However, WT mice treated with curare showed a marked (~50%) reduction in shivering but were able to maintain an average core temperature of 35.4 ± 0.4 °C, which is close to the optimal core temperature, suggesting that NST mechanisms are sufficient for the maintenance of core temperature in the absence of shivering (Supplementary Fig. 2b and Supplementary Video 2). Next, we minimized shivering with curare in iBAT-ablated WT mice to highlight the existence of muscle-based NST. Notably, iBAT-ablated WT mice were able to maintain their core temperature when exposed to 4 °C, and treatment with curare did not cause any significant additional decrease (35.1 ± 0.5 °C) (Fig. 2c), suggesting that skeletal-muscle–based NST is an important mechanism for thermoregulation. We then investigated whether blunting of shivering by treatment with curare affects thermogenesis in *Sln*$^{-/-}$ mice with intact iBAT. Notably, reduction of shivering by curare treatment caused a rapid decline in core temperature in these mice during the first hour of exposure (37.1 ± 0.4 °C to 34.5 ± 0.8 °C in 30 min and then to 33.9 ± 0.9 °C in 60 min) (Fig. 2d,e). These data indicate that shivering is an important component of thermoregulation during the initial phase of cold challenge. Curare treatment only modestly altered physical activity, but the treated mice were able to move around freely and showed normal grooming behavior (Fig. 2f). Further, measurements of VO_2 in WT and *Sln*$^{-/-}$ mice during cold challenge showed that treatment with curare did not affect metabolic rate (Supplementary Fig. 2c,d).

To show the role of Ryr1-mediated Ca^{2+} leak in Sln-mediated NST, we used dantrolene, an inhibitor of Ryr commonly used to treat malignant hyperthermia[26]. Administration of dantrolene (4 mg per kg body weight intraperitoneally) did not affect physical activity, including shivering, in WT mice with and without intact iBAT and *Sln*$^{-/-}$ mice with intact iBAT exposed to 4 °C (Supplementary Fig. 3a), but in WT mice with intact iBAT pretreated with dantrolene and exposed to 4 °C, core temperature decreased to 34.6 ± 0.4 °C (Fig. 3a). Similarly, treatment of iBAT-ablated WT mice with dantrolene caused a significant ($P <$ 0.001) decrease in their average core temperature to 33.0 ± 1.0 °C (Fig. 3a). However, treatment with dantrolene had little effect on *Sln*$^{-/-}$ mice, as they were already cold sensitive (Fig. 3b). These data may suggest that Ryr1-mediated Ca^{2+} leak could be involved in increasing the cytoplasmic calcium pool that is essential for stimulating thermogenesis through Serca. VO_2 was increased after cold challenge in WT mice with and without intact iBAT and *Sln*$^{-/-}$ mice with intact iBAT pretreated with dantrolene (Supplementary Fig. 3b).

Although previous studies have suggested that the Serca pump can generate heat[27,28] during Ca^{2+} transport, the exact mechanism of this process has not been explored. To determine

how the Sln interaction with Serca leads to heat generation, we compared the interaction of Sln and Serca to that of phospholamban (Plb), a known regulator of the Serca pump, by chemical crosslinking using microsomes from HEK 293 cells in the presence of increasing concentrations of Ca^{2+}. We introduced cysteine at a homologous position, as determined by a comparison of the amino acid sequences of Sln and Plb, to create a site for crosslinking (Fig. 3c). Previous studies have shown that N30C Plb specifically crosslinks with Serca, and by screening the N-terminal residues of Sln for crosslinking with Serca[29], we found E7C Sln, homologous to N30C Plb, specifically crosslinks with Serca. Crosslinking studies with bismaleimidohexane (BMH, a homobifunctional sulfhydryl crosslinker) showed that Sln harboring the E7C mutation continues to interact with Serca even in the presence of high concentrations of Ca^{2+} (0.1–100 μM) (Fig. 3d). However, the interaction of Plb harboring the N30C mutation with Serca is abolished at concentrations of Ca^{2+} above 0.1 μM, as has been previously reported[29] (Fig. 3e). This finding showing that Sln and Ca^{2+} can bind to Serca simultaneously suggests that Sln has the ability to promote uncoupling of the pump, leading to increased ATP hydrolysis and heat production.

We next tested whether the presence of Sln results in increased energy cost by challenging $Sln^{-/-}$ mice with a high-fat diet (HFD) at 22 ± 1.5 °C for 12 weeks. HFD feeding resulted in significantly more weight gain in $Sln^{-/-}$ mice compared to WT mice (Fig. 4a,b) despite a lower food (weight and calorie) intake (Supplementary Fig. 4). $Sln^{-/-}$ mice had higher fat content, as determined by magnetic resonance imaging (MRI) (2.55-fold ± 0.33-fold) (mean ± s.e.m.) and fat pad weights, than WT mice (Fig. 4c,d). Further, a histological analysis showed that white adipose tissue, BAT and liver cells of HFD-fed $Sln^{-/-}$ mice had more fat droplet accumulation than those of WT mice (Fig. 4e). HFD-fed WT mice were less obese than $Sln^{-/-}$ mice (Fig. 4a and Supplementary Fig. 5) but had upregulated Sln expression (3-fold to 5-fold in the soleus), suggesting that Sln-mediated NST is recruited to increase metabolism (Fig. 4f), but the expressions of Serca1a and Serca2a were not altered in these mice. HFD-fed $Sln^{-/-}$ mice showed elevated serum glucose, cholesterol and triglyceride concentrations and elevated glucose intolerance (Fig. 4g and Supplementary Fig. 4c,d). We also found an upregulation of Ucp1 expression in the BAT of both HFD-fed groups, as reported previously[30] (Supplementary Fig. 5b), and the expressions of Serca and Sln were not altered in cardiac muscle by HFD (Supplementary Fig. 5c). These data provide evidence that Sln-Serca–based NST is recruited during metabolic overload to increase energy expenditure, thereby reducing adiposity.

In conclusion, our findings show that skeletal muscle is an important site of NST and the SLN-SERCA interaction is the basis for skeletal-muscle thermogenesis. We suggest that SLN-mediated NST in the maintenance of core temperature is central in animals that have reduced BAT content[6,31] or in which functional BAT is absent (birds[32] and pigs[33]). These findings are relevant to large mammals, including humans, where SLN is expressed several fold higher than in rodents[34] and BAT content becomes restricted in adult life[35]. Based on these findings, we propose that the SLN-SERCA interaction in skeletal muscle can serve as a potential target to modulate energy metabolism and treat metabolic-overload–induced obesity.

METHODS

Mice

The generation of *Sln*$^{-/-}$ mice has been described previously[36]. Sln over-expression in mouse skeletal muscle was achieved using the skeletal α-actin promoter[37]. The transgenic line 4, with protein overexpression in skeletal muscle but not other tissues, was selected for further breeding with the *Sln*$^{-/-}$ mice to generate *Sln*$^{-/-/OE}$ mice. The genotypes of the mice were determined by PCR from tail snips, and all mice were maintained in the C57BL/6J genetic background. The study protocol was approved by the Ohio State University Institutional Animal Care and Use Committee (OSU-IACUC). All of the animal procedures were carried out at our Association for Assessment and Accreditation of Laboratory Animal Care International–accredited animal facility and conducted in accordance with the Guide for the Care and Use of Laboratory Animals.

iBAT removal surgery and measurements of core temperature

Surgical removal of iBAT was performed under anesthesia according to OSU-IACUC–approved protocols. A 1- to 2-cm incision was made on the dorsal skin, the iBAT was removed by dissection, and the skin was closed with wound clips. Control mice underwent similar surgery except without removal of iBAT. Mice were allowed to fully recover before they were challenged to 4 °C. The core body temperature of the mice was measured using telemetric transponders (IPTT-300, BioMedic Data System Inc, Seaford, DE, USA) implanted just below the skin in the interscapular region. The whole-body core temperature was calculated as the mean temperature from each group between 2 and 4 h after cold challenge. The surface temperature of the mice was imaged using a high-resolution infrared camera (Ti32-60HZ Thermal Imager, Fluke Corporation, Everett, WA, USA).

Acute cold challenge

Acute cold exposure of mice to 4 °C was performed in the CLAMS (CLAMS Columbus Instruments Inc, Columbus, OH, USA) set up, which is temperature controlled. For these experiments, 12-week-old male mice were individually housed, and their core temperature was measured using telemetric transponders. Metabolic parameters (oxygen consumption and carbon dioxide production) were monitored throughout the experiment by indirect calorimetry. In addition, the physical activity of each mouse was monitored using a multidimensional infrared light detection system placed on bottom and top levels of each individual cage of the CLAMS. Age-matched WT and *Sln*$^{-/-}$ mice were acclimatized to 30.0 ± 1.0 °C for 3 weeks, and the mice were challenged to acute cold at 4 °C as described above. Shivering in WT and *Sln*$^{-/-}$ mice was recorded for 1 h during the 4 °C cold challenge, and representative stretches of these recordings are presented as Supplementary Videos 1 and 2.

Treatment with curare and dantrolene

Curare and dantrolene were solubilized in an aqueous solution containing 0.9% NaCl and administered intraperitoneally. Curare (D-tubocurarine hydrochloride, Sigma-Aldrich, St. Louis, MO, USA) was administered at 0.4 mg per kg body weight, as previously reported[38]. Dantrolene (dantrolene sodium salt, Sigma-Aldrich, St. Louis, MO, USA) was administered

at 4 mg per kg body weight, as previously reported[39]. After administration of the drug, the mice were visually monitored for 15 min and then transferred to the CLAMS for acute cold challenge. The number of shivering episodes (>5 s) was quantified for 1 h in the curare-treated mice ($n = 4$) during cold challenge.

Chemical crosslinking of Sln with Serca

Complementary DNA (cDNA) of rat Serca1 and mouse Sln and Plb were cloned into the pcDNA 3.1(+) vector between the restriction sites NheI and XhoI, and EcoRI and XhoI, respectively. The residues in the Sln (Glu7) and Plb (Asn30) sequences were mutated to cysteine for crosslinking through the QuikChangeTM site-directed mutagenesis method (Stratagene, La Jolla, CA). Serca1 cDNA with E7C Sln or N30C Plb cDNA was co-transfected into cultured HEK 293 cells using lipofectamine, and microsomes were prepared as described previously[40] after 48 h of transfection. Chemical crosslinking was performed using the homobifunctional sulfhydryl crosslinker BMH (Thermo Scientific Inc., Rockford, IL, USA) as described previously[41]. The reaction mixture contained 40 mM 3-(N-morpholino)propa nesulfonic acid (MOPS) (pH 7.0), 3.2 mM $MgCl_2$, 75 mM KCl, 3mM ATP and 1 mM ethylene glycol tetraacetic acid (EGTA). The calculation of free calcium was done by Maxchelator freeware, and $CaCl_2$ was added to make the desired amount of free calcium in the reaction. Individual reactions contained 15 μg of microsome, and the reaction was started by adding 0.1 mM BMH and then incubating for 1 h. The reaction was stopped by adding SDS-PAGE sample-loading buffer containing 15% SDS with 100 mM dithiothretol. Crosslinked samples were subjected to SDS-PAGE and standard western blotting using antibodies to Sln (custom made, 1:2,000 dilution), Plb (Zymed 1:3,000 dilution) and Serca1a (custom made, 1:2,000 dilution).

HFD-induced obesity

Eight-week-old $Sln^{-/-}$ mice and WT littermates (age and weight matched) were segregated into four experimental groups and fed either a standard chow diet (3.0 kcal/g, 4.25% kCal from fat) or an HFD (4.73 kcal/g, 45% kCal from fat; D12451, Research Diet Inc., New Brunswick, NJ, USA). Body weight was measured once every week and was expressed as weight gained in grams per mouse. Body fat distribution was measured by nuclear magnetic resonance using a 9.4T system (Bruker BioSpin, Billerica, MA, USA) in our Small Animal Imaging Facility. The mice were anaesthetized with 1–1.5% isoflurane and secured on an animal bed inside the MRI scanner. The mice were monitored using a small animal monitoring system (Model 1025, Small Animals Instruments, Inc. Stony Brook, NY, USA), and the heart rates of the mice were maintained in the range 350–450 beats per minute by adjusting the amount of the anesthesia. To further confirm the MRI results, the fat pads were weighed and expressed as a percentage of the total body weight.

Serum chemistry

Serum chemistry in HFD-fed mice was performed after overnight fasting. Serum glucose was measured using Breeze 2 glucometer (Bayer HealthCare LLC, Tarrytown, NY, USA). Serum triglyceride, cholesterol and ketone were measured using a CardioChek PA kit (HealthCheck Systems, Brooklyn, NY, USA). Glucose tolerance tests were performed on fasted mice (12 h) by intraperitoneal injection of 3-glucose (2 g per kg of body weight).

Western blotting

Expression of Sln, Serca1a, Serca2a (custom-made antibodies, 1:3,000 dilution), Casq1 (Affinity bioreagents antibody to Casq1, MA3913, 1:1,000 dilution) and Ucp1 (Abcam, ab10983, 1:2,000 dilution) were determined using standard western blotting techniques. The desired amount of whole homogenate supernatant was adequately resolved by SDS-PAGE (16% Tris-tricine gel for Sln and 8% or 10% Tris-glycine gel for other proteins). Proteins were transferred to a 0.2-μM nitrocellulose membrane for Sln or a 0.45-μM nitrocellulose membrane for the other proteins and blocked with 5% milk or BSA containing 0.05% Tween 20 for 60 min. Secondary horseradish-peroxidase–conjugated antibody (KPL Inc., 074-1506) was applied for 1 h at room temperature at a dilution of 1:50,000 in Tris-buffered saline containing 0.05% Tween-20. Signal was detected using an enhanced chemiluminescence reagent (Pierce Thermo Scientific). The protein bands were then scanned (HP Imaging).

Statistical analyses

Data are expressed as means ± s.e.m. Statistically significant differences between two groups were assessed by Student's *t* test or one-way ANOVA.

Supplementary Material

Refer to Web version on PubMed Central for supplementary material.

Acknowledgments

This work was supported in part by US National Institutes of Health grant R01 (HL080551) to M. Periasamy. N.C.B. was supported by a postdoctoral fellowship from the American Physiological Society and the American Heart Association (10POST3360007). This work was also supported in part by research grants from the Canadian Institutes of Health Research to A.R.T. (MOP 86618 and MOP 47296). We thank P. Mohler, J.A. Rafael-Fortney and J.E. Ostler, for comments on the manuscript. We thank N. Manivannan and K. Powell (Ohio State University Medical Center, Davis Heart and Lung Research Institute, Small Animal Imaging Facility, Columbus, Ohio, USA) for MRI of mice.

References

1. Asahi M, et al. Cardiac-specific overexpression of sarcolipin inhibits sarco(endo)plasmic reticulum Ca^{2+} ATPase (SERCA2a) activity and impairs cardiac function in mice. Proc Natl Acad Sci USA. 2004; 101:9199–9204. [PubMed: 15201433]
2. Asahi M, et al. Sarcolipin regulates sarco(endo)plasmic reticulum Ca^{2+}-ATPase (SERCA) by binding to transmembrane helices alone or in association with phospholamban. Proc Natl Acad Sci USA. 2003; 100:5040–5045. [PubMed: 12692302]
3. Babu GJ, et al. Targeted overexpression of sarcolipin in the mouse heart decreases sarcoplasmic reticulum calcium transport and cardiac contractility. J Biol Chem. 2006; 281:3972–3979. [PubMed: 16365042]
4. Babu GJ, et al. Ablation of sarcolipin enhances sarcoplasmic reticulum calcium transport and atrial contractility. Proc Natl Acad Sci USA. 2007; 104:17867–17872. [PubMed: 17971438]
5. Babu GJ, et al. Overexpression of sarcolipin decreases myocyte contractility and calcium transient. Cardiovasc Res. 2005; 65:177–186. [PubMed: 15621045]
6. Block BA. Thermogenesis in muscle. Annu Rev Physiol. 1994; 56:535–577. [PubMed: 8010751]
7. Silva JE. Physiological importance and control of non-shivering facultative thermogenesis. Front Biosci (Schol Ed). 2011; 3:352–371. [PubMed: 21196381]

8. Enerbäck S, et al. Mice lacking mitochondrial uncoupling protein are cold-sensitive but not obese. Nature. 1997; 387:90–94.
9. Dawkins MJ, Scopes JW. Non-shivering thermogenesis and brown adipose tissue in the human newborn infant. Nature. 1965; 206:201–202.
10. Cannon B, Nedergaard J. Metabolic consequences of the presence or absence of the thermogenic capacity of brown adipose tissue in mice (and probably in humans). Int J Obes (Lond). 2010; 34 (suppl 1):S7–S16. [PubMed: 20935668]
11. Kjelstrup S, Barragan D, Bedeaux D. Coefficients for active transport and thermogenesis of Ca^{2+}-ATPase isoforms. Biophys J. 2009; 96:4376–4386. [PubMed: 19486662]
12. Anunciado-Koza RP, et al. Inactivation of the mitochondrial carrier SLC25A25 (ATP-Mg^{2+}/Pi transporter) reduces physical endurance and metabolic efficiency in mice. J Biol Chem. 2011; 286:11659–11671. [PubMed: 21296886]
13. Block BA, Franzini-Armstrong C. The structure of the membrane systems in a novel muscle cell modified for heat production. J Cell Biol. 1988; 107:1099–1112. [PubMed: 3417775]
14. Block BA, O'Brien J, Meissner G. Characterization of the sarcoplasmic reticulum proteins in the thermogenic muscles of fish. J Cell Biol. 1994; 127:1275–1287. [PubMed: 7962089]
15. Morrissette JM, Franck JP, Block BA. Characterization of ryanodine receptor and Ca^{2+}-ATPase isoforms in the thermogenic heater organ of blue marlin (*Makaira nigricans*). J Exp Biol. 2003; 206:805–812. [PubMed: 12547935]
16. da Costa DC, Landeira-Fernandez AM. Thermogenic activity of the Ca^{2+}-ATPase from blue marlin heater organ: regulation by KCl and temperature. Am J Physiol Regul Integr Comp Physiol. 2009; 297:R1460–R1468. [PubMed: 19710387]
17. MacLennan DH. Ca^{2+} signalling and muscle disease. Eur J Biochem. 2000; 267:5291–5297. [PubMed: 10951187]
18. Smith WS, Broadbridge R, East JM, Lee AG. Sarcolipin uncouples hydrolysis of ATP from accumulation of Ca^{2+} by the Ca^{2+}-ATPase of skeletal-muscle sarcoplasmic reticulum. Biochem J. 2002; 361:277–286. [PubMed: 11772399]
19. Mall S, et al. The presence of sarcolipin results in increased heat production by Ca^{2+}-ATPase. J Biol Chem. 2006; 281:36597–36602. [PubMed: 17018526]
20. Tupling AR, et al. Enhanced Ca^{2+} transport and muscle relaxation in skeletal muscle from sarcolipin-null mice. Am J Physiol Cell Physiol. 2011; 301:C841–C849. [PubMed: 21697544]
21. Hofmann WE, Liu X, Bearden CM, Harper ME, Kozak LP. Effects of genetic background on thermoregulation and fatty acid–induced uncoupling of mitochondria in UCP1-deficient mice. J Biol Chem. 2001; 276:12460–12465. [PubMed: 11279075]
22. Vitali A, et al. The adipose organ of obesity-prone C57BL/6J mice is composed of mixed white and brown adipocytes. J Lipid Res. 2012; 53:619–629. [PubMed: 22271685]
23. Lim S, et al. Cold-induced activation of brown adipose tissue and adipose angiogenesis in mice. Nat Protoc. 2012; 7:606–615. [PubMed: 22383039]
24. Kashimura O, Sakai A, Yanagidaira Y, Ueda G. Thermogenesis induced by inhibition of shivering during cold exposure in exercise-trained rats. Aviat Space Environ Med. 1992; 63:1082–1086. [PubMed: 1456920]
25. Bowman WC. Neuromuscular block. Br J Pharmacol. 2006; 147 (suppl 1):S277–S286. [PubMed: 16402115]
26. Wang R, et al. Localization of the dantrolene-binding sequence near the FK506-binding protein-binding site in the three-dimensional structure of the ryanodine receptor. J Biol Chem. 2011; 286:12202–12212. [PubMed: 21262961]
27. Kjelstrup S, de Meis L, Bedeaux D, Simon JM. Is the Ca^{2+}-ATPase from sarcoplasmic reticulum also a heat pump? Eur Biophys J. 2008; 38:59–67. [PubMed: 18679670]
28. de Meis L, Arruda AP, Carvalho DP. Role of sarco/endoplasmic reticulum Ca^{2+}-ATPase in thermogenesis. Biosci Rep. 2005; 25:181–190. [PubMed: 16283552]
29. Jones LR, Cornea RL, Chen Z. Close proximity between residue 30 of phospholamban and cysteine 318 of the cardiac Ca^{2+} pump revealed by intermolecular thiol cross-linking. J Biol Chem. 2002; 277:28319–28329. [PubMed: 12015326]

30. Rippe C, Berger K, Boiers C, Ricquier D, Erlanson-Albertsson C. Effect of high-fat diet, surrounding temperature, and enterostatin on uncoupling protein gene expression. Am J Physiol Endocrinol Metab. 2000; 279:E293–E300. [PubMed: 10913028]

31. Arruda AP, et al. Cold tolerance in hypothyroid rabbits: role of skeletal muscle mitochondria and sarcoplasmic reticulum Ca^{2+} ATPase isoform 1 heat production. Endocrinology. 2008; 149:6262–6271. [PubMed: 18703625]

32. Bicudo JE, Vianna CR, Chaui-Berlinck JG. Thermogenesis in birds. Biosci Rep. 2001; 21:181–188. [PubMed: 11725866]

33. Berg F, Gustafson U, Andersson L. The uncoupling protein 1 gene (*UCP1*) is disrupted in the pig lineage: a genetic explanation for poor thermoregulation in piglets. PLoS Genet. 2006; 2:e129. [PubMed: 16933999]

34. Babu GJ, Bhupathy P, Carnes CA, Billman GE, Periasamy M. Differential expression of sarcolipin protein during muscle development and cardiac pathophysiology. J Mol Cell Cardiol. 2007; 43:215–222. [PubMed: 17561107]

35. Cypess AM, et al. Identification and importance of brown adipose tissue in adult humans. N Engl J Med. 2009; 360:1509–1517. [PubMed: 19357406]

36. Babu GJ, et al. Ablation of sarcolipin enhances sarcoplasmic reticulum calcium transport and atrial contractility. Proc Natl Acad Sci USA. 2007; 104:17867–17872. [PubMed: 17971438]

37. Brennan KJ, Hardeman EC. Quantitative analysis of the human α-skeletal actin gene in transgenic mice. J Biol Chem. 1993; 268:719–725. [PubMed: 7678010]

38. Kashimura O, Sakai A, Yanagidaira Y, Ueda G. Thermogenesis induced by inhibition of shivering during cold exposure in exercise-trained rats. Aviat Space Environ Med. 1992; 63:1082–1086. [PubMed: 1456920]

39. Dainese M, et al. Anesthetic- and heat-induced sudden death in calsequestrin-1– knockout mice. FASEB J. 2009; 23:1710–1720. [PubMed: 19237502]

40. Jones LR, Cornea RL, Chen Z. Close proximity between residue 30 of phospholamban and cysteine 318 of the cardiac Ca^{2+} pump revealed by intermolecular thiol cross-linking. J Biol Chem. 2002; 277:28319–28329. [PubMed: 12015326]

41. Maruyama K, MacLennan DH. Mutation of aspartic acid-351, lysine-352, and lysine-515 alters the Ca^{2+} transport activity of the Ca^{2+}-ATPase expressed in COS-1 cells. Proc Natl Acad Sci USA. 1988; 85:3314–3318. [PubMed: 2966962]

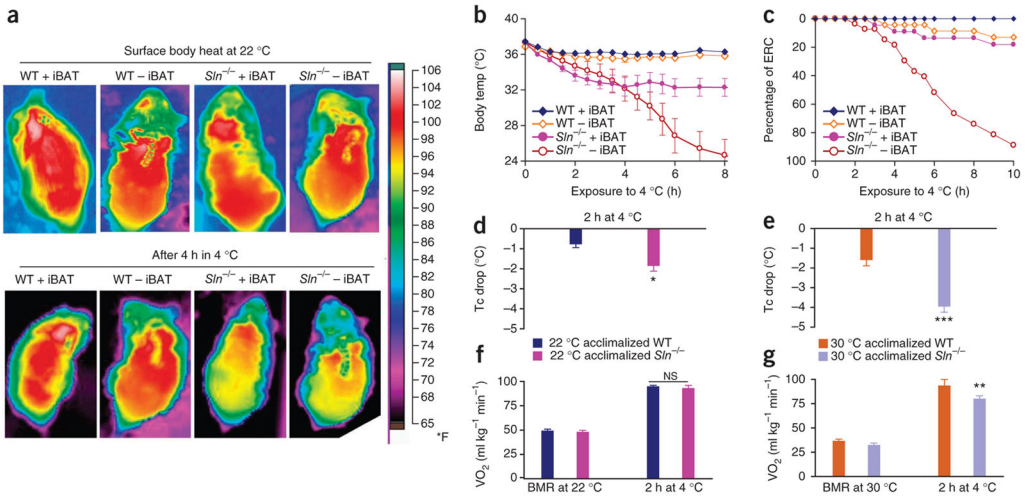

Figure 1.

Sln$^{-/-}$ mice are not able to maintain optimal core temperature (~37 °C) and develop hypothermia when challenged with acute cold. (**a**) Infrared imaging of surface body heat in WT and *Sln*$^{-/-}$ mice with or without iBAT at 22 °C and 4 °C. (**b**) Core body temperature after acute cold exposure in WT and *Sln*$^{-/-}$ mice, with and without iBAT. $n = 22$ (WT + iBAT), $n = 23$ (WT – iBAT), $n = 22$ (*Sln*$^{-/-}$ + iBAT), $n = 27$ (*Sln*$^{-/-}$ – iBAT). (**c**) Percentage of mice reaching ERC. (**d**,**e**) Average drop in core temperature (Tc) during the first 2 h of 4 °C challenge in WT and *Sln*$^{-/-}$ mice first acclimatized to 22 °C (**d**) or 30 °C (**e**). (**f**,**g**) Oxygen consumption averaged over the first two hours of acute cold exposure in WT and *Sln*$^{-/-}$ mice first acclimatized to 22 °C (**f**) or 30 °C (**g**). *$P < 0.05$, **$P < 0.01$, ***$P < 0.001$, NS, not significant as analyzed by Student's *t* test or one-way analysis of variance (ANOVA). All data are means ± s.e.m.

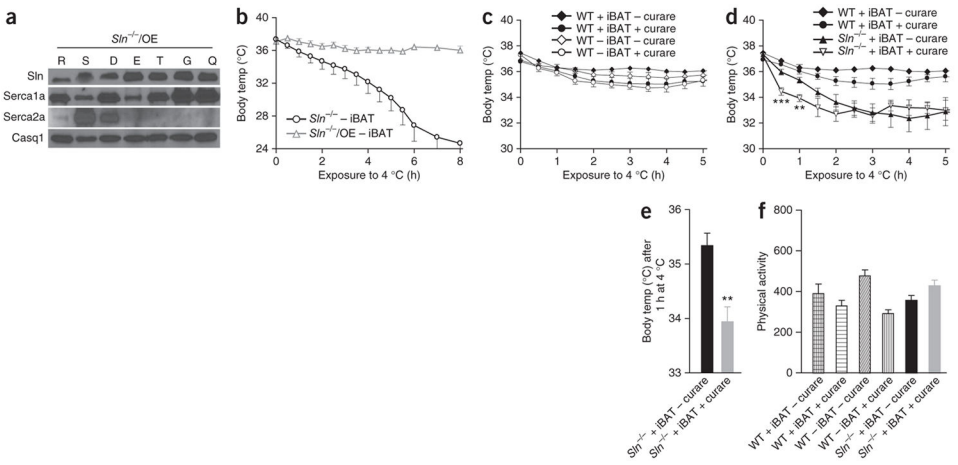

Figure 2.

Reintroduction of *Sln* in $Sln^{-/-}$ mice completely restores thermogenesis, and Sln is necessary for muscle-based NST. (**a**) Transgenic overexpression of Sln in $Sln^{-/-/OE}$ mice. R, red gastrocnemius; S, soleus; D, diaphragm; E, extensor digitorum longus; T, tibialis anterior; G, gastrocnemius; Q, quadriceps; Casq1, skeletal calsequestrin. (**b**) Core body temperature during acute cold exposure after *Sln* overexpression in the $Sln^{-/-}$ ($n = 8$) background. (**c**–**e**) Core body temperature during acute cold exposure in WT mice (**c**) and in $Sln^{-/-}$ mice (**d**,**e**) after curare treatment. (**f**) Physical activity of the indicated mouse strains with and without curare treatment. $^{**}P < 0.01$, $^{***}P < 0.001$ by Student's *t* test. All data are means ± s.e.m.

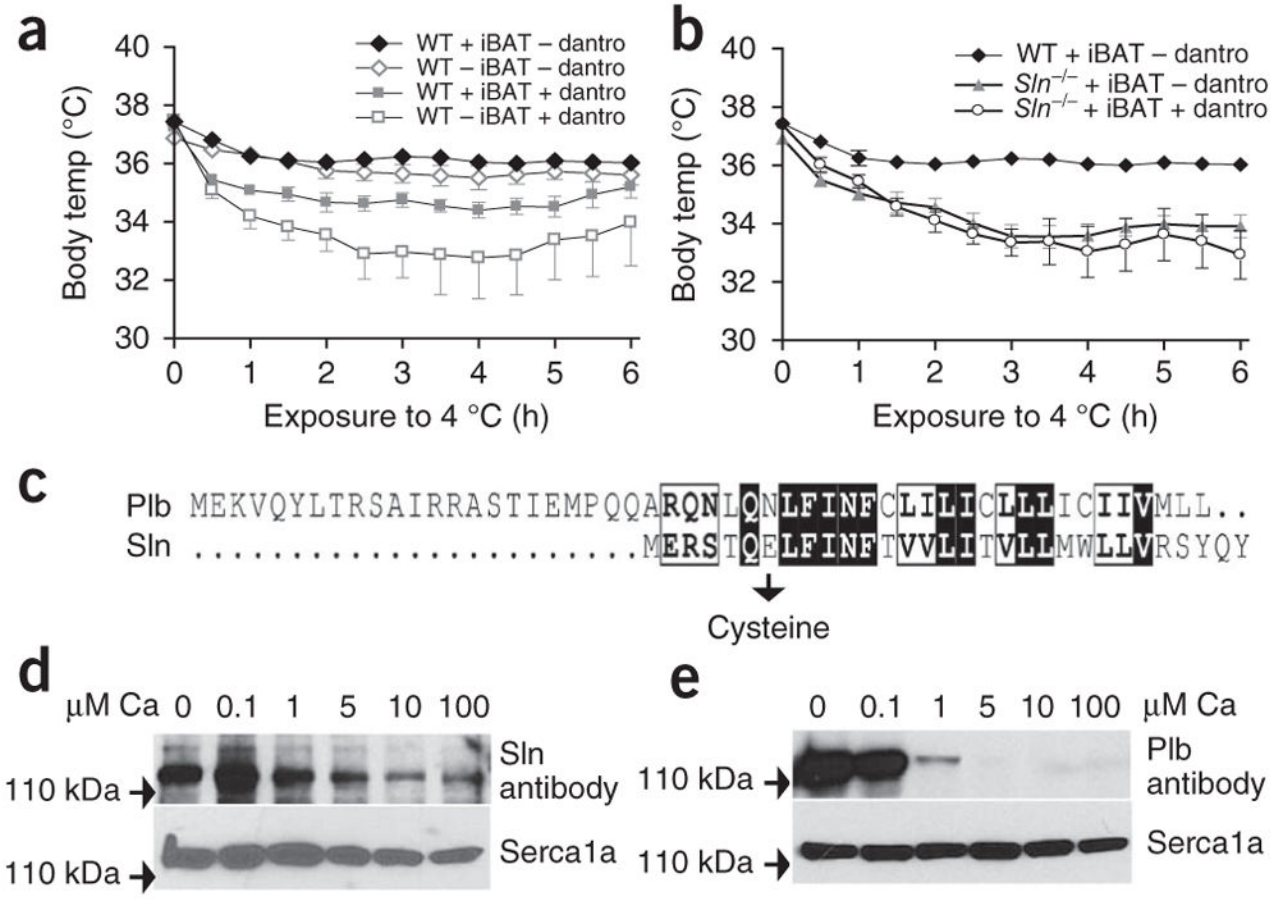

Figure 3.

Molecular basis of Sln-mediated thermogenesis. (**a**,**b**) Core body temperature after acute cold exposure and after dantrolene treatment in WT mice (**a**) and $Sln^{-/-}$ mice (**b**) with or without iBAT. $n = 8$ (WT + iBAT), $n = 8$ (WT – iBAT), $n = 11$ ($Sln^{-/-}$ + iBAT). (**c**) Alignment of the mouse Sln and Plb protein sequences. The amino acid residues Asp30 in Plb and Glu7 in Sln were mutated to cysteine for crosslinking experiments with Serca1a. (**d**) Western blot analysis showing Sln crosslinking to Serca1a in the presence of Ca^{2+} (0 –100 µM). (**e**) Western blot showing crosslinking of Plb with Serca1a in the presence of Ca^{2+} (0 – 100 µM). All data are means ± s.e.m.

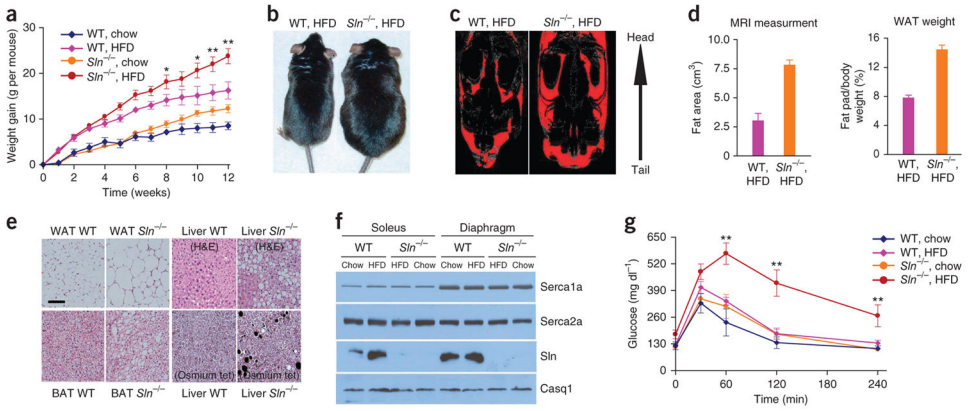

Figure 4.

$Sln^{-/-}$ mice are prone to develop obesity when fed HFD. (**a**) Increase in body weight during 12 weeks of HFD feeding ($n = 8$ mice per group). (**b**) $Sln^{-/-}$ mice fed HFD become obese compared to WT mice. (**c**) MRI of the fat distribution in representative mice fed on HFD. (**d**) Determination of the fat content of the mice in **a**. WAT, white adipose tissue. (**e**) Representative histological sections of intraperitoneal WAT, BAT and liver stained with H&E and osmium tetroxide (osmium tet) (seen as black dots). Scale bar, 25 μm. (**f**) Representative western blots of soleus and diaphragm muscle from chow-fed and HFD-fed WT and $Sln^{-/-}$ mice. $n = 4$. (**g**) Glucose tolerance test. $^{*}P < 0.05$, $^{**}P < 0.01$ for the comparison of WT and $Sln^{-/-}$ HFD-fed mice by one-way ANOVA. All data are means ± s.e.m.